Multi-dimensional quasi-discrete model for the investigation of heating and evaporation of Diesel fuel droplets

Mansour Al Qubeissi*, Sergei S Sazhin, Guillaume de Sercey, Cyril Crua
Sir Harry Ricardo Laboratories, School of Computing, Engineering and Mathematics,
University of Brighton, Brighton BN2 4GJ, UK
*Corresponding author: m.alqubeissi@brighton.ac.uk

Abstract

Previously developed droplet heating and evaporation models, taking into account temperature gradient, recirculation, and species diffusion within droplets, and their application to the analysis of commercial automotive fuel droplets are reviewed. It is shown that the most efficient analysis of Diesel fuel droplet heating and evaporation is based on the MDQD (multi-dimensional quasi-discrete) model, taking into account the contribution of all groups of hydrocarbons in automotive fuels. The main features of this model are summarised and its new application to the analysis of droplets in Diesel engine-like conditions, taking into account time-dependent velocities, is described. In the MDQD model, Diesel fuel is approximated by six groups of components: alkanes, cycloalkanes, bicycloalkanes, alkylbenzenes, indanes & tetralines, naphthalenes, and three characteristic components $C_{19}H_{34}$ (tricycloalkane), $C_{13}H_{12}$ (diaromatic), and $C_{14}H_{10}$ (phenanthrene). It is shown that errors in estimated temperatures and evaporation times in typical Diesel engine conditions, using the approximation of Diesel fuel by 15 quasi-components/components compared to the case when all 98 components are taken into account, are up to 1% and 3%, respectively. This is acceptable in most engineering applications. This approximation has also reduced CPU time by about 6 times compared with the case when the contribution of 98 components is taken into account. The approximations of Diesel fuel with n-dodecane (widely used in engineering modelling) and 20 alkane components lead to under-prediction of the evaporation time by over 50% and 22%, respectively.

Introduction

Diesel fuel droplet heating and evaporation are crucial processes leading to fuel auto-ignition and combustion in internal combustion engines. The accuracy of modelling of these processes is important for improving the design of these engines [1–3]. Various approaches to the modelling of fuel droplet heating and evaporation are discussed in [1–14].

Previous studies have mainly focused on two approaches to modelling multi-component droplet heating and evaporation. The focus of the first approach is on the analysis of individual components. These models are known as Discrete Multi-Component (DMC), or Discrete Component Models (DCM) [15–22]; they are applicable in the case when a small number of components needs to be taken into account. The focus of the second approach is on the probabilistic analysis of a large number of components, as in the case of the Continuous Thermodynamics (CT) approach [23–30] and the Distillation Curve Model [31–33]. In this family of models a number of additional simplifying assumptions have been used, including the assumption that species inside droplets mix infinitely quickly (Infinite Diffusivity model) or do not mix at all (single-component model). These assumptions are shown to be too crude for modelling realistic automotive fuel droplets [4,7,14,34–36].

An approach, combining some features of the above-mentioned approaches is suggested in [10,11]. These papers describe a methodology for the representation of fuels using a lumping procedure combined with adequate thermodynamic and thermophysical models. Such a procedure allows the computation of various thermodynamic and thermophysical properties for simulation purposes in internal combustion engines. This approach involves reducing analytical data to a few pseudo-components characterised by their molecular weight, critical properties and acentric factor (real gas effects were taken into account in this model).

The quasi-discrete (QD) model suggested in [14], and further developed in [34], has some similarities with the pseudo-component model described in [10,11]. One of the key advantages of the QD model, compared with the pseudo-component model, is that the former takes into account the diffusion of quasi-components and thermal diffusion inside droplets. The analysis of [14,34] is based on the assumption that the dominant components in automotive fuels are alkanes. Large numbers of alkane components have been replaced by a relatively small number of Quasi-Components (QC) without compromising the accuracy of calculations. The QD model, however, has a number of serious limitations, such as the assumption that Diesel and gasoline fuels consist only of n-alkanes and the distribution of these components can be approximated by a relatively simple distribution function. In our recent paper [8], the

quasi-discrete model has been generalised to take into account the other groups of Diesel fuels in addition to alkanes. These groups can be categorised according to the similarity in the physical and chemical behaviour of their components. In the next section, the main ideas of the models described in [14,34,8] are summarised. Then, the model described in [8] is applied to a more realistic case than the one considered in the original paper, where it is no longer assumed that droplet velocities are constant.

The model

The model used in our analysis takes into account species diffusion inside droplets and finite liquid thermal conductivity. Also, recirculations (vortices) in droplets due to the relative velocity between ambient gas and droplets are taken into account. The latter effect is taken into account by replacing the finite species diffusivity and finite liquid thermal conductivity with Effective Diffusivity (ED) and Effective Thermal Conductivity (ETC), respectively. This model is known as the ED/ETC model [2,3,6]. In the original quasi-discrete model (see [14,34]), the contribution of various n-alkanes is described by the distribution function $f_m(n)$:

$$f_m(n) = C_m(n_0, n_f)\frac{(M(n)-\gamma)^{\alpha-1}}{\beta^{\alpha}\,\Gamma(\alpha)}\,\exp\left[-\left(\frac{M(n)-\gamma}{\beta}\right)\right], \tag{1}$$

where n is the number of carbon atoms, $n_0 \le n \le n_f$, subscripts $_0$ and $_f$ stand for initial and final, M is molar mass, $\Gamma(\alpha)$ is the Gamma function, α and β are parameters determining the shape of the distribution function, γ determines the original shift, and constant C_m is defined as:

$$C_m = \left\{\int_{M_1}^{M_2}\frac{(M-\gamma)^{\alpha-1}}{\beta^{\alpha}\Gamma(\alpha)}\exp\left[-\left(\frac{M-\gamma}{\beta}\right)\right]dM\right\}^{-1}. \tag{2}$$

This expression for C_m follows from the requirement that:

$$\int_{M_1}^{M_2} f_m(M)\,dM = 1. \tag{3}$$

Assuming that the properties of hydrocarbons in a certain narrow range of n are close, the continuous distribution $f_m(M)$ can be replaced with a discrete one, consisting of N_f Quasi-Components (QC) with carbon numbers:

$$\bar{n}_j = \frac{\int_{n_{j-1}}^{n_j} n\, f_m(n)\,\mathrm{d}n}{\int_{n_{j-1}}^{n_j} f_m(n)\,\mathrm{d}n}, \tag{4}$$

and the corresponding molar fractions:

$$X_j = \int_{n_{j-1}}^{n_j} f_m(n)\,\mathrm{d}n, \tag{5}$$

where j is an integer in the range $(1 \le j \le N_f)$. Note that:

$$\sum_{j=1}^{j=N_f} X_j = 1. \tag{6}$$

The choice of n_j could be arbitrary. It was assumed that all $n_j - n_{j-1}$ are equal, i.e. all QC have the same range of values of n. For the case when $N_f = 1$ this approach reduces the analysis of multi-component droplets to that of mono-component droplets. These new QC are not the actual physical hydrocarbon components ($\bar{n}_j$ in Equation (5) are not integers in the general case). Hence, this model was called a 'quasi-discrete' model. These QC are treated as the actual components in the conventional DMC model, including taking into account the diffusion of liquid QC in droplets. This model was expected to be particularly useful when N_f is much less than the number of actual species in the hydrocarbon mixture.

There are two main problems with the application of the QD approach to realistic Diesel fuels, the composition of which is shown in Figure 1. Firstly, even if the analysis is restricted only to alkanes, it does not appear to be easy to approximate this distribution with a reasonably simple distribution function $f_m(n)$, given by Expression (1). Secondly,

the contributions of the other nine hydrocarbon-groups apart from n-alkanes (see Figure 1), cannot be ignored in any realistic model of Diesel fuels. In the model suggested in [8] both of these issues are addressed.

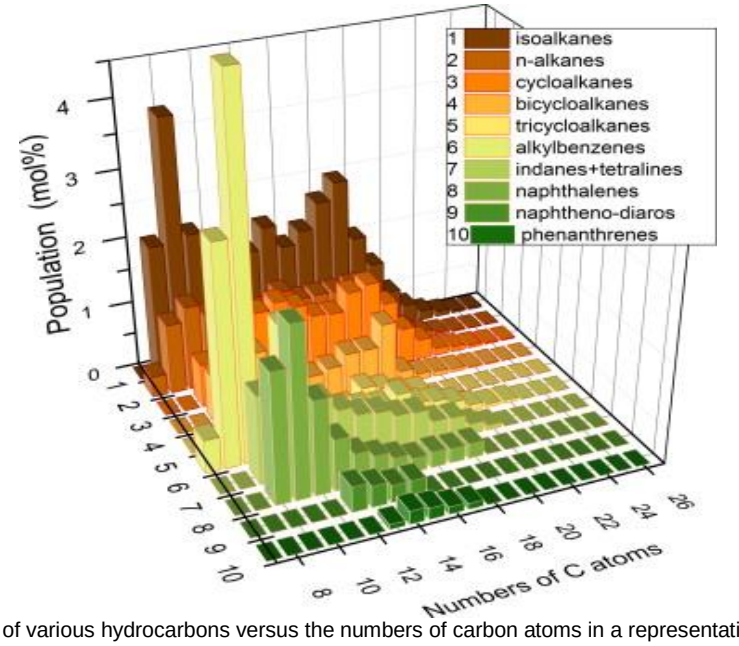

Figure 1. Molar fractions of various hydrocarbons versus the numbers of carbon atoms in a representative sample of commercial Diesel fuel. Reprinted from [37], Copyright Elsevier (2013).

These are the molar fractions of each group of species, shown in Figure 1: 13.6518% n-alkanes, 26.4039% iso-alkanes, 14.8795% cycloalkanes, 7.6154% bicycloalkanes, 1.5647% tricycloalkanes, 16.1719% alkylbenzenes, 9.1537% indanes & tetralines, 8.6773% naphthalenes, 1.2240% diaromatics, and 0.6577% phenanthrenes. For simplicity, n-alkanes and iso-alkanes are treated as one group of alkanes due to small differences between their thermodynamic properties. The detailed composition of this fuel, apart from tricycloalkanes, diaromatics and phenanthrenes, is given in Table 1 [8,37].

Table 1. Molar fractions of components for Diesel fuel shown in Figure 1.

Number of Carbon atoms	Alkanes	Cyclo-alkanes	Bicyclo-alkanes	Alkyl-benzenes	Indanes & Tetralines	Naphthalenes
C8	0.308	0	0	0.497	0	0
C9	3.032	0	0	3.2357	0	0
C10	5.0541	0.6408	0.6926	5.3584	1.3157	1.9366
C11	3.163	1.8745	1.0524	0.9492	1.3632	2.529
C12	2.6156	1.6951	0.9753	1.9149	1.1951	1.4012
C13	2.5439	1.2646	0.6611	0.6873	1.0652	0.7692
C14	2.6497	1.3633	0.5631	0.6469	0.8406	0.4879
C15	3.1646	1.2353	0.4314	0.4782	0.7051	0.3843
C16	2.6579	1.0449	0.4921	0.4564	0.6684	0.2854
C17	2.8605	1.0162	0.6529	0.4204	0.5598	0.2072
C18	3.2403	1.2848	0.6554	0.5234	0.5357	0.2358

C19	3.5296	1.3566	0.9901	0.3226	0.3403	0.2151
C20	2.2338	0.9961	0.1965	0.2848	0.3227	0.2256
C21	1.443	0.5374	0.0935	0.2032	0.1638	0
C22	0.799	0.304	0.0701	0.0969	0.0781	0
C23	0.3972	0.109	0.0488	0.0494	0	0
C24	0.1903	0.0755	0.0234	0.0473	0	0
C25	0.0997	0.0445	0.0169	0	0	0
C26	0.0425	0.0214	0	0	0	0
C27	0.0309	0.0155	0	0	0	0

The groups with very small contributions (up to 1.5%), tricycloalkanes, diaromatics, and phenanthrenes, were replaced with individual characteristic components $C_{19}H_{34}$ (tricycloalkane), $C_{13}H_{12}$ (diaromatic), and $C_{14}H_{10}$ (phenanthrene). Hence, Diesel fuel can be represented with six groups of species and 3 characteristic components.
In the new model, the focus is shifted from the analysis of the distribution function to the direct analysis of molar fractions of the components. These are described by the matrix X_{nm}, where n refers to the number of carbon atoms, and m refers to the groups (e.g. alkanes) or individual characteristic components (tricycloalkane, diaromatic and phenanthrene). The link between the values of m and the groups of components is shown in Table 2.

Table 2. The Diesel fuel groups of components.

m	Group	Molar fraction (%)
1	alkanes	40.0556
2	cycloalkanes	14.8795
3	bicycloalkanes	7.6154
4	alkylbenzenes	16.1719
5	indanes & tetralines	9.1537
6	naphthalenes	8.6773
7	tricycloalkane	1.5647
8	diaromatic	1.2240
9	phenanthrene	0.6577

For each m the values of $\bar{n}_{jm}$ of each QC can be introduced as:

$$\left.\begin{aligned}
\bar{n}_{1_m} &= \frac{\sum_{n=n_{1m}}^{n=n_{(\varphi_m+1)m}} (nX_{nm})}{\sum_{n=n_{1m}}^{n=n_{(\varphi_m+1)m}} X_{nm}},\\
\bar{n}_{2_m} &= \frac{\sum_{n=n_{(\varphi_m+2)_m}}^{n=n_{(2\varphi_m+2)m}} (nX_{nm})}{\sum_{n=n_{(\varphi_m+2)_m}}^{n=n_{(2\varphi_m+2)m}} X_{nm}},\\
\bar{n}_{3_m} &= \frac{\sum_{n=n_{(2\varphi_m+3)_m}}^{n=n_{(3\varphi_m+3)m}} (nX_{nm})}{\sum_{n=n_{(2\varphi_m+3)_m}}^{n=n_{(3\varphi_m+3)m}} X_{nm}},\\
&\vdots\\
\bar{n}_{l_m} &= \frac{\sum_{n=n_{((\ell-1)\varphi_m+\ell)_m}}^{n=n_{k_m}} (nX_{nm})}{\sum_{n=n_{((\ell-1)\varphi_m+\ell)_m}}^{n=n_{k_m}} X_{nm}},
\end{aligned}\right\} \qquad (7)$$

where $n_{1m} = n_{m(\min)}$ is the minimal value of n for which $X_{nm} \neq 0$, $n_{km} = n_{m(\max)}$ is the maximal value of n for which $X_{nm} \neq 0$, and $\ell = \text{integer}((k_m + \varphi_m)/(\varphi_m + 1))$. Parameter φ_m is assumed to be integer; $\varphi_m + 1$ is equal to the number of components to be included within each quasi-component, except possibly the last one in the group. φ_m is

assumed to be the same for all QC within group m. If $\varphi_m = 0$ then $\ell = k_m$ and the number of QC is equal to the number of actual components. φ_m and k_m depend on m in the general case.
As in the case of the original QD model, $\bar{n}_{im}$ are not integers in the general case. In the case when mass fractions of Components/Quasi-Components (C/QC) with large carbon numbers are small, these C/QC can be merged to form single QC. Due to the additional dimensions introduced by the subscript m in Equation (8), the new model is called the 'Multi-Dimensional Quasi-Discrete' (MDQD) model. The minimal number of $\bar{n}_{im}$ for the groups shown in Table 2 is 9 (when $\varphi_m = k_m - 1$ for all m). As in [8], in the current study, optimum reductions in the number of QCs, provided that the errors introduced by this reduction are acceptable for practical engineering applications, are investigated. The molar fractions of these C/QC are estimated as:

$$\left.\begin{aligned} X_{1_m} &= \sum_{n=n_{1m}}^{n=n_{(\varphi_m+1)m}} X_{nm}, \\ X_{2_m} &= \sum_{n=n_{(\varphi_m+2)_m}}^{n=n_{(2\varphi_m+2)m}} X_{nm}, \\ &\vdots \\ X_{3_m} &= \sum_{n=n_{((\ell-1)\varphi_m+\ell)_m}}^{n=n_{k_m}} X_{nm}, \end{aligned}\right\} \qquad (8)$$

Note that in the case when the maximal $\ell = k_m$, the new approach reduces to the conventional DMC model.

Results and Discussion

The multi-dimensional quasi-discrete model, described in the previous section was applied to the analysis of heating and evaporation of Diesel fuel droplets of an initial radius R_{d0}= 10 μm and initial temperature T_0= 300 K. The ambient gas temperature and pressure were assumed constant and equal to 880 K and 3 MPa, respectively. These input parameters have been implemented from the conditions used in [8], which are close to those used in [9,33,39] and observed in [38]. The velocities of the droplets observed in [38] varied in the range U_d= 10-35 m/s. The observed and approximated time-dependence of these velocities are shown in Figure 2.

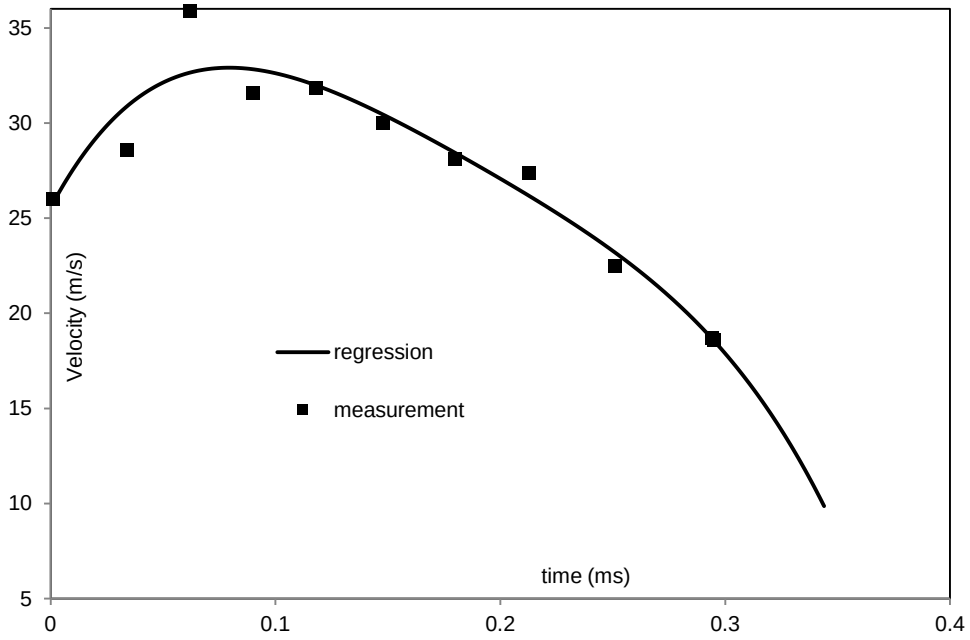

Figure 2. The measured and approximated droplet velocities in the SMD region.

The velocities plotted in Figure 2 are derived from the panorama images of the spray interface described in [38]. For each position in the panorama, 20 image pairs were captured 700 ms after the start of injection, with a delay of 500 ns between the two images of the pair. From each image pair, velocity vectors were computed using a basic single pass PIV (Particle Image Velocimetry) algorithm with constant cell size. The first image of a pair and the resulting velocity vectors are shown in Figure 3.

The velocity vectors were then averaged for each axial position of the spray to obtain a single average velocity per position. Since the injection mass flow rate was in steady-state at the timing of acquisition, the axial positions were then converted into time, based on the calculated average velocities. The furthest measurement was at 25 mm from the nozzle, corresponding to a total transit time of 0.4 ms. The velocities of droplets at times greater than 0.4 ms were assumed equal to those at 0.4 ms. Simultaneously, the droplet SMD was determined using the dropsizing technique described in [38].

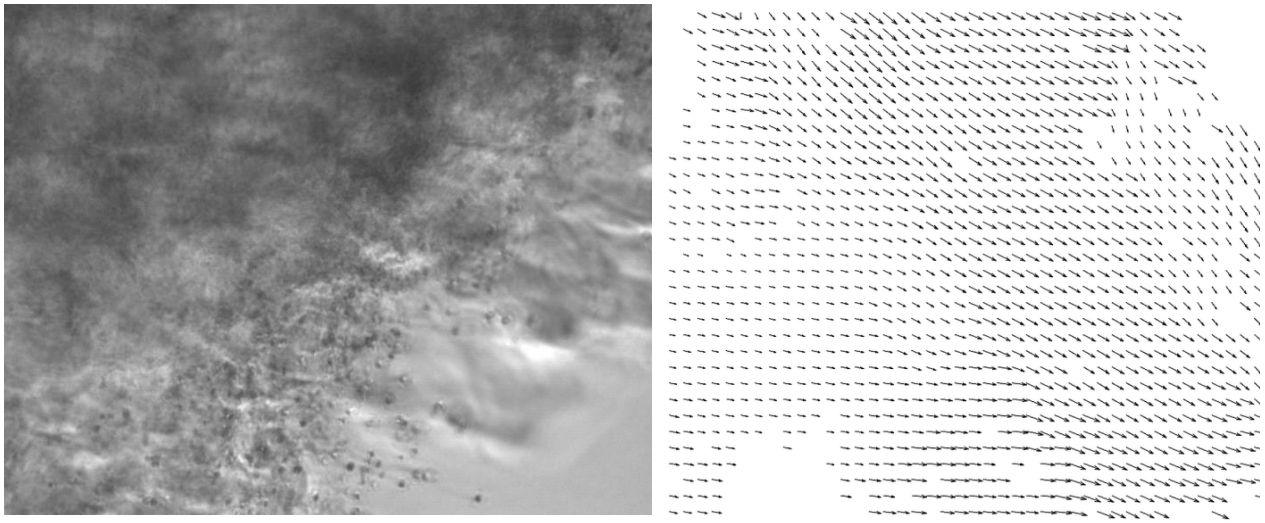

Figure 3. Spray image (23 mm from the nozzle) and resulting velocity vectors.

The measured velocities, shown in Figure 2, were approximated by the following expression to facilitate their input to the model:

$$U_d = -9658.1\,t^4 + 7288.7\,t^3 - 2140.9\,t^2 + 221.5\,t + 25.553 \quad (9)$$

The plots of the droplet surface temperatures T_s and radii R_d versus time for various approximations of Diesel fuel composition are shown in Figure 4. These plots illustrate 4 cases: the contributions of all 98 components are taken into account (labelled “(98)”); the contributions of only 20 alkane components, shown in Tables 1 and 2, are taken into account (standard approximation used in the original QD model [14,34]) (labelled “(20A)”); the contributions of all 98 components are approximated by 15 C/QC; and the contribution of only n-dodecane is taken into account.

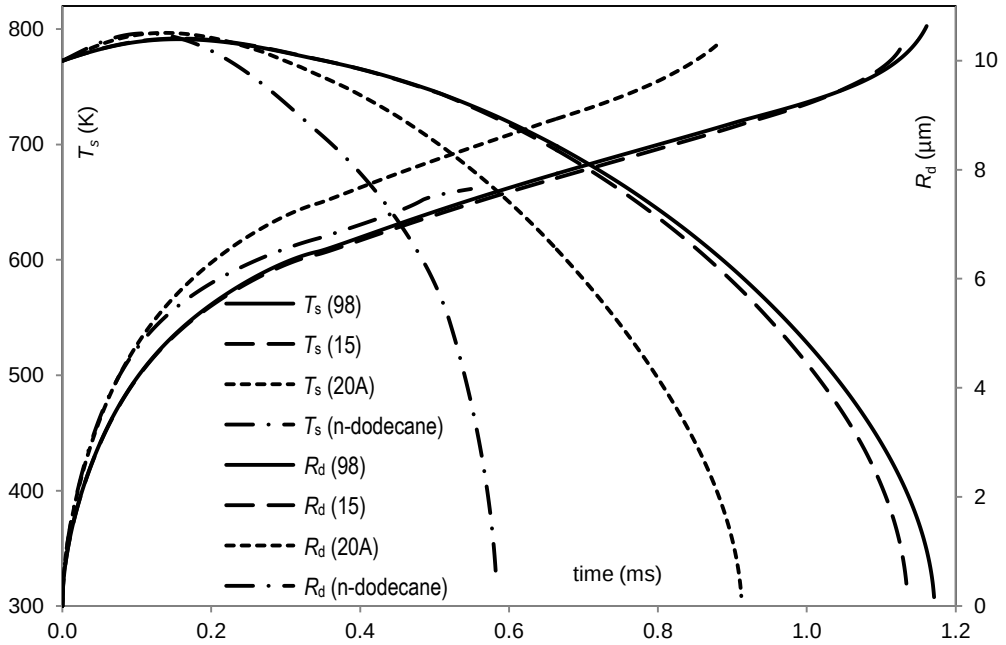

Figure 4. The droplet surface temperatures T_s and radii R_d versus time for three approximations of Diesel fuel composition, taking into account the contributions of all 98 components (98); 20 alkane components (20A),15 C/QC (15); and treating Diesel fuel as n-dodecane.

The mass fractions of various components at the surface of the droplet versus time, for the case when Diesel fuel is approximated with 15 C/QC, are shown in Figure 5. As can be seen from this figure, the surface mass fractions of the lightest QCs, $C_{10.335}H_{22.670}$, $C_{10.207}H_{14.413}$, and $C_{12.495}H_{16.990}$, decrease with time, while the surface mass fraction of the heaviest QC, $C_{22.977}H_{45.953}$, increases with time.

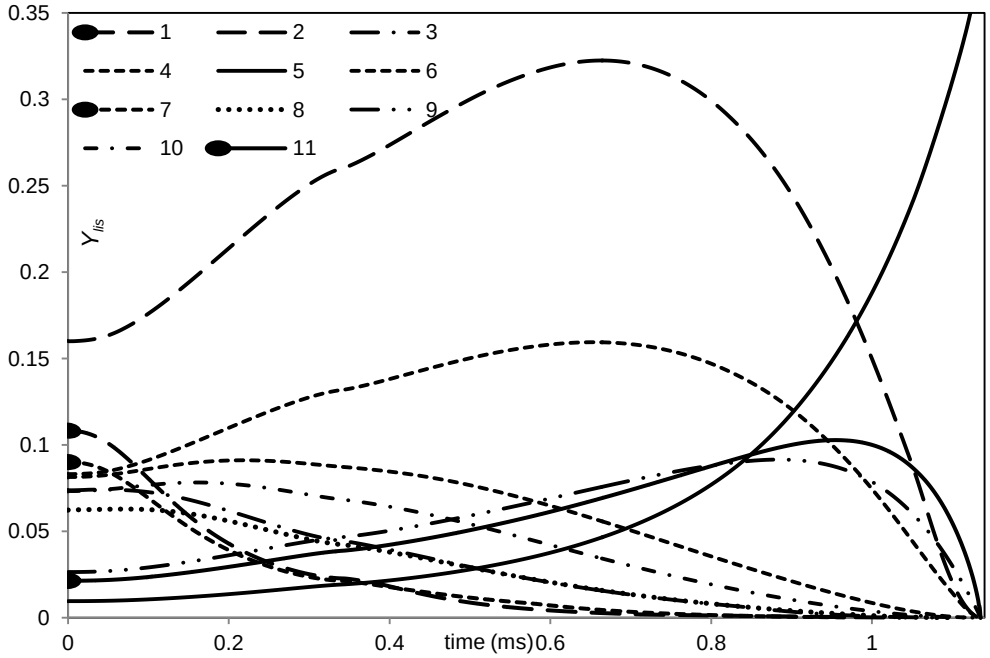

Figure 5. The surface mass fractions Y_{lis} of 11 characteristic and/or dominant C/QC, predicted from the model taking into account the contributions of 15 C/QC; these are the C/QC: alkane $C_{10.335}H_{22.670}$ (range $C_8H_{18} - C_{12}H_{26}$) (1), alkane $C_{19.380}H_{40.760}$ (range $C_{18}H_{38} - C_{22}H_{46}$) (2), cycloalkane $C_{12.562}H_{25.125}$ (range $C_{10}H_{20} - C_{15}H_{30}$) (3), cycloalkane $C_{18.297}H_{36.595}$ (range $C_{16}H_{32} - C_{21}H_{42}$) (4), cycloalkane $C_{22.977}H_{45.953}$ (range $C_{22}H_{44} - C_{27}H_{54}$) (5), bicycloalkane $C_{14.743}H_{27.487}$ (range $C_{10}H_{18} - C_{25}H_{48}$) (6), alkylbenzene $C_{10.207}H_{14.413}$ (range $C_8H_{10} - C_{13}H_{20}$) (7), indane or tetraline $C_{12.495}H_{16.990}$ (range $C_{10}H_{12} - C_{16}H_{24}$) (8), indane or tetraline $C_{18.615}H_{29.229}$ (range $C_{17}H_{26} - C_{22}H_{36}$) (9), naphthalene $C_{12.392}H_{12.783}$ (range $C_{10}H_8 - C_{20}H_{28}$) (10), tricycloalkane $C_{19}H_{34}$ (11).

The effect of temperature gradient inside the droplet is illustrated in Figure 6 for three time instants.

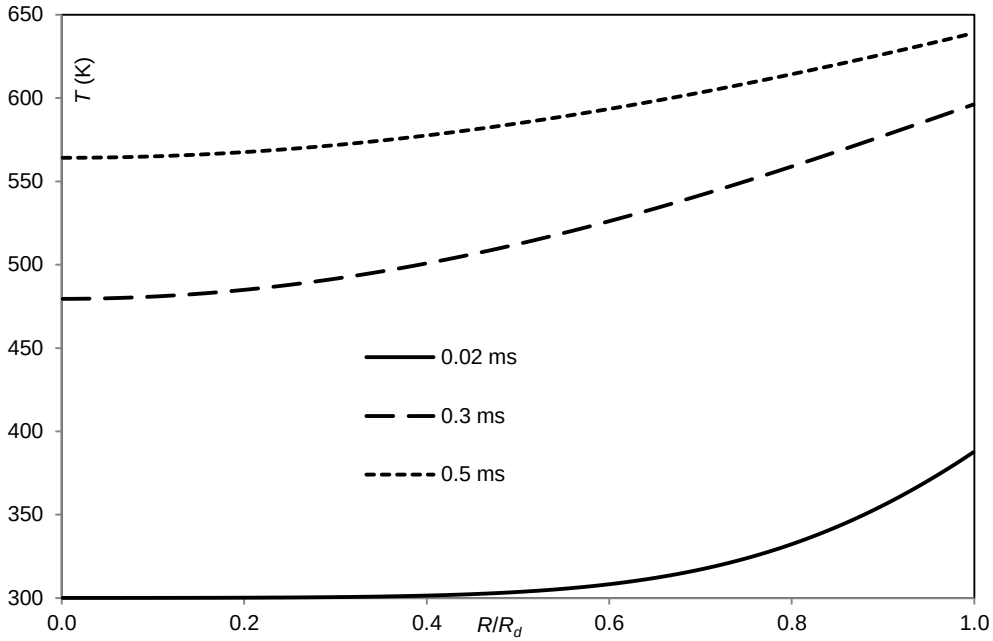

Figure 6. The plots of temperature versus normalised distance from the droplet centre (R/R_d) at three instants of time 0.02 ms, 0.3 ms and 0.5 ms (indicated near the plots) as predicted by the model, taking into account the contributions of 15 C/QC.

The effect of species mass fraction gradient, at three time instants, is illustrated in Figure 7.

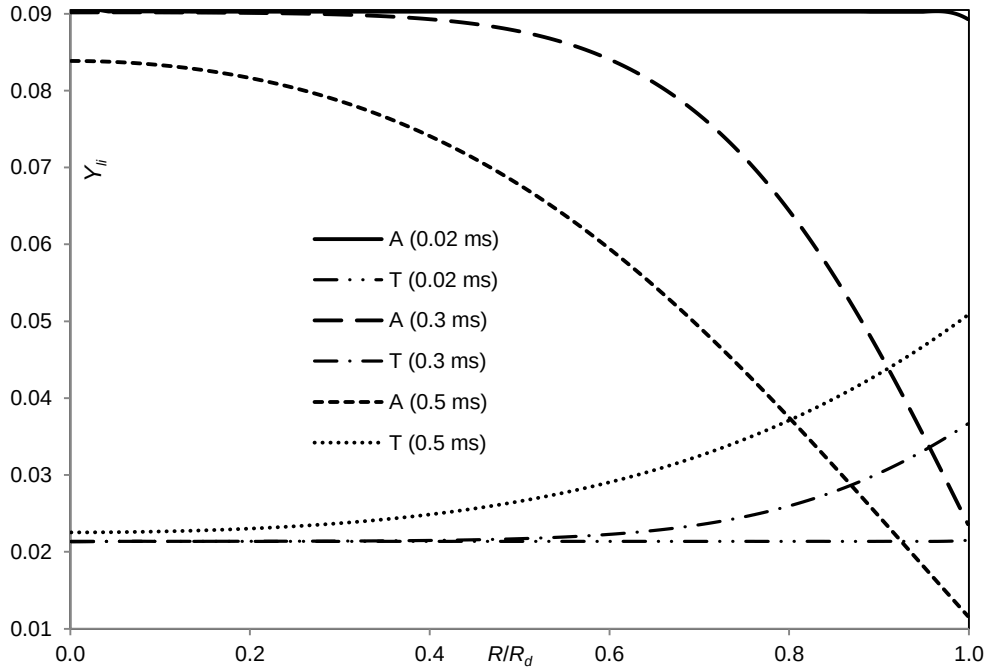

Figure 7. Mass fractions of alkylbenzene QC $C_{10.207}H_{14.413}$ (range $C_8H_{10} - C_{13}H_{20}$) and tricycloalkane $C_{19}H_{34}$, versus normalised distance from the droplet centre (R/R_d) at three time instants, 0.02 ms, 0.3 ms and 0.5 ms (indicated near the plots), predicted by the model based on the approximation of Diesel fuel by 15 C/QC.

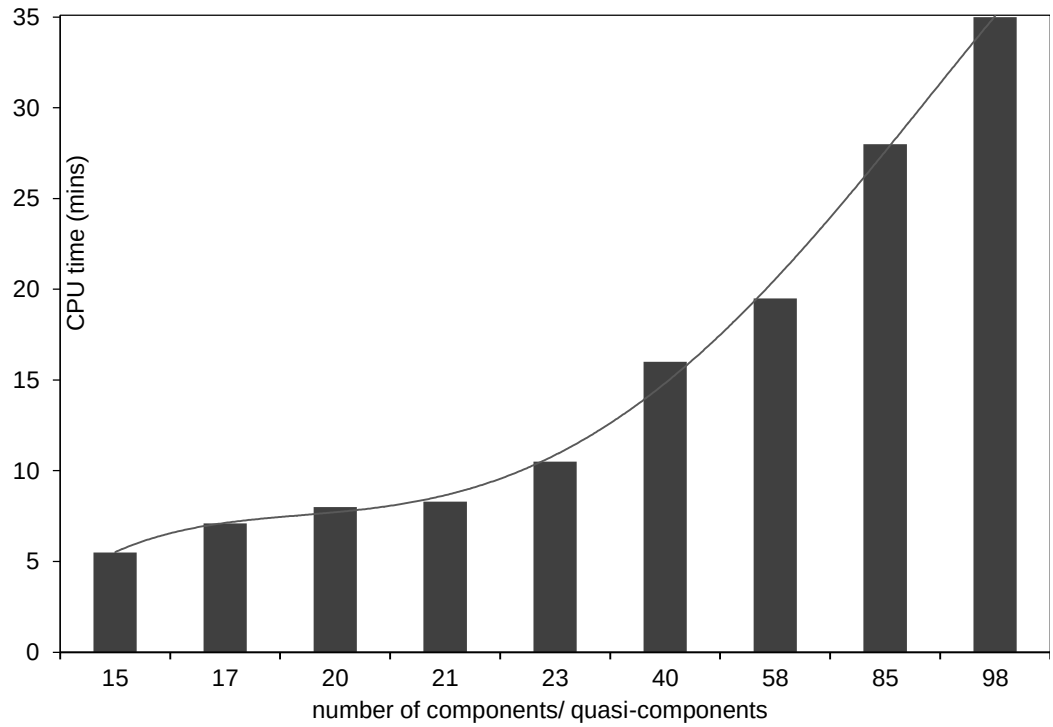

Figure 8. The plot of CPU time, required for calculations of droplet heating and evaporation, versus the number of C/QC used in the model.

As shown in Figure 4, the approximations of Diesel fuel by 20 alkane components and a single (n-dodecane) component lead to under-estimation of droplet evaporation time by more than 22% and 50%, respectively, which are not acceptable in many engineering applications. At the same time, the approximation of 98 components of Diesel fuel by 15 quasi-components/components leads to under-prediction of this time by less than 3%, which can be acceptable in most applications. Also, approximating 98 components of Diesel fuel by 15 C/QC, requires about 1/6th of the CPU time compared with the model taking into account the contributions of all 98 components, as shown in Figure 8.

Acknowledgements

The authors are grateful to the European Regional Development Fund [INTERREG IVa project 'E3C3', grant number 4274] for financial support.

Nomenclature

f_m	Distribution function of components [-]
m	Groups or components [-]
M	Molar mass [-]
n	Carbon number [-]
N_f	Number of quasi-components [-]
R	Distance from the centre of the droplet [m]
R_d	Droplet radius [µm]
t	Time [s]
T_s	Temperature at the surface of the droplet [K]
X	Molar fraction [-]
Y_{lis}	Mass fractions of liquid species at the surface of the droplet [-]

Abbreviations

C/QC	Components/Quasi-Components
CFD	Computational Fluid Dynamics
CPU	Central Processing Unit
CT	Continuous Thermodynamics
DC	Discrete Components

DMC Discrete Multi-Component
ETC Effective Thermal Conductivity
ED Effective Diffusivity
MDQD Multi-Dimensional Quasi-Discrete
SMD Sauter Mean Diameter
QC Quasi Components
QD Quasi-Discrete

References

[1] Abramzon, B., and Sazhin, S. S., 2006, Fuel, **85**(1), pp. 32–46.
[2] Sazhin, S. S., 2014, Droplets and sprays, Springer-Verlag, London.
[3] Sirignano, W. A., 1999, Fluid dynamics and transport of droplets and sprays, Cambridge University Press.
[4] Al Qubeissi, M., Kolodnytska, R., and Sazhin, S. S., 2013, 25th European Conference on Liquid Atomization and Spray Systems, Crete, Greece.
[5] Abramzon, B., and Sazhin, S., 2005, International Journal of Heat and Mass Transfer, **48**(9), pp. 1868–1873.
[6] Sazhin, S. S., 2006, Progress in Energy and Combustion Science, **32**(2), pp. 162–214.
[7] Sazhin, S. S., Al Qubeissi, M., Kolodnytska, R., Elwardany, A. E., Nasiri, R., and Heikal, M. R., 2014, Fuel, **115**, pp. 559–572.
[8] Sazhin, S. S., Al Qubeissi, M., Nasiri, R., Gunko, V. M., Elwardany, A. E., Lemoine, F., Grisch, F., and Heikal, M. R., 2014, Fuel, **129**, pp. 238-266.
[9] Elwardany, A. E., Gusev, I. G., Castanet, G., Lemoine, F., and Sazhin, S. S., 2011, Atomization and Sprays, **21**(11), pp. 907–931.
[10] Lugo, R., Ebrahimian, V., Lefebvre, C., Habchi, C., and de Hemptinne, J.-C., 2010, SAE, **2010-01-2183**.
[11] Habchi, C., Lafossas, F. A., Béard, P., and Broseta, D., 2004, SAE, **2004-01-1996**.
[12] Sazhin, S. S., Elwardany, A., Krutitskii, P. A., Castanet, G., Lemoine, F., Sazhina, E. M., and Heikal, M. R., 2010, International Journal of Heat and Mass Transfer, **53**(21-22), pp. 4495–4505.
[13] Sazhina, E. M., Sazhin, S. S., Heikal, M. R., Babushok, V. I., and Johns, R. J. R., 2000, Combustion Science and Technology, **160**(1), pp. 317–344.
[14] Sazhin, S. S., Elwardany, A. E., Sazhina, E. M., and Heikal, M. R., 2011, International Journal of Heat and Mass Transfer, **54**(19-20), pp. 4325–4332.
[15] Abraham, J., and Magi, V., 1998, SAE, **980511**.
[16] Aggarwal, S. K., and Mongia, H. C., 2002, Journal of Engineering for Gas Turbines and Power, **124**(2), p. 248.
[17] Continillo, G., and Sirignano, W. A., 1991, Modern Research Topics in Aerospace Propulsion, G. Angelino, L.D. Luca, and W.A. Sirignano, eds., Springer New York, pp. 173–198.
[18] Klingsporn, M., and Renz, U., 1994, International Journal of Heat and Mass Transfer, **37**, pp. 265–272.
[19] Lage, P. L. C., Hackenberg, C. M., and Rangel, R. H., 1995, Combustion and Flame, **101**(1-2), pp. 36–44.
[20] Maqua, C., Castanet, G., and Lemoine, F., 2008, Fuel, **87**(13-14), pp. 2932–2942.
[21] Ra, Y., and Reitz, R. D., 2009, International Journal of Multiphase Flow, **35**(2), pp. 101–117.
[22] Tong, A. Y., and Sirignano, W. A., 1986, Numerical Heat Transfer, **10**(3), pp. 253–278.
[23] Abdel-Qader, Z., and Hallett, W. L. H., 2005, Chemical Engineering Science, **60**(6), pp. 1629–1640.
[24] Arias-Zugasti, M., and Rosner, D. E., 2003, Combustion and Flame, **135**(3), pp. 271–284.
[25] Hallett, W. L. H., 2000, Combustion and Flame, **121**(1-2), pp. 334–344.
[26] Lippert, A. M., and Reitz, R. D., 1997, Modeling of Multicomponent Fuels Using Continuous Distributions with Application to Droplet Evaporation and Sprays, SAE International, Warrendale, PA.
[27] Rivard, E., and Brüggemann, D., 2010, Chemical Engineering Science, **65**(18), pp. 5137–5145.
[28] Tamim, J., and Hallett, W. L. H., 1995, Chemical Engineering Science, **50**(18), pp. 2933–2942.
[29] Zhang, L., and Kong, S.-C., 2009, Chemical Engineering Science, **64**(16), pp. 3688–3696.
[30] Zhu, G.-S., and Reitz, R. D., 2002, International Journal of Heat and Mass Transfer, **45**(3), pp. 495–507.
[31] Burger, M., Schmehl, R., Prommersberger, K., Schäfer, O., Koch, R., and Wittig, S., 2003, International Journal of Heat and Mass Transfer, **46**(23), pp. 4403–4412.
[32] Ott, L. S., Smith, B. L., and Bruno, T. J., 2010, American Journal of Environmental Sciences, **6**(6), pp. 523–534.
[33] Smith, B. L., and Bruno, T. J., 2006, Int J Thermophys, **27**(5), pp. 1419–1434.
[34] Elwardany, A. E., and Sazhin, S. S., 2012, Fuel, **97**, pp. 685–694.
[35] Elwardany, A. E., 2012, PhD thesis, University of Brighton.
[36] Elwardany, A. E., Sazhin, S. S., and Farooq, A., 2013, Fuel, **111**, pp. 643–647.
[37] Gun'ko, V. M., Nasiri, R., Sazhin, S. S., Lemoine, F., and Grisch, F., 2013, Fluid Phase Equilibria, **356**, pp. 146–156.
[38] Crua, C., de Sercey, G., Gold, M., and Heikal, M. R., 2013, 25th European Conference on Liquid Atomization and Spray Systems, Chania, Greece.
[39] Kolodnytska, R., Al Qubeissi, M., and Sazhin, S. S., 2013, 25th European Conference on Liquid Atomization and Spray Systems, Crete, Greece.